Optics Letters

Experimental demonstration of tunable homodyne detection of WDM and dual-polarization PSK channels by automatically locking the channels to a local pump laser using nonlinear mixing

Ahmed Almaiman,[1,*] Morteza Ziyadi,[1] Amirhossein Mohajerin-Ariaei,[1] Yinwen Cao,[1] Mohammad Reza Chitgarha,[1] Peicheng Liao,[1] Changjing Bao,[1] Bishara Shamee,[1] Nisar Ahmed,[1] Fatemeh Alishahi,[1] Ahmad Fallahpour,[1] Youichi Akasaka,[2] Jeng-Yuan Yang,[2] Motoyoshi Sekiya,[2] Joseph D. Touch,[1,3] Moshe Tur,[4] Carsten Langrock,[5] Martin M. Fejer,[5] and Alan E. Willner[1]

[1]Department of Electrical Engineering, University of Southern California, Los Angeles, California 90089, USA
[2]Fujitsu Laboratories of America, 2801 Telecom Parkway, Richardson, Texas 75082, USA
[3]Information Sciences Institute, University of Southern California, 4676 Admiralty Way, Marina del Rey, California 90292, USA
[4]School of Electrical Engineering, Tel Aviv University, Ramat Aviv 69978, Israel
[5]Edward L. Ginzton Laboratory, Stanford University, Stanford, California 94305, USA
*Corresponding author: Almaiman@usc.edu

Received 4 April 2016; revised 3 May 2016; accepted 10 May 2016; posted 11 May 2016 (Doc. ID 262494); published 2 June 2016

This Letter proposes a method for tunable automatically locked homodyne detection of wavelength-division multiplexing (WDM) dual-polarization (DP) phase-shift keyed (PSK) channels using nonlinear mixing. Two stages of periodically poled lithium niobate (PPLN) waveguides and an LCoS filter enable automatic phase locking of the channels to a local laser. © 2016 Optical Society of America

OCIS codes: (060.2360) Fiber optics links and subsystems; (190.4223) Nonlinear wave mixing.

http://dx.doi.org/10.1364/OL.41.002680

Coherent optical communication systems using dual-polarization (DP) phase-shift keyed (PSK) formats have gained considerable interest for encoding data over wavelength-multiplexed links due to their high spectral efficiency and the ability to use digital signal post-processing to compensate for various data-degrading effects [1–3]. Optical homodyne detection is known to provide better performance and is optimally 3 dB more sensitive than optical heterodyne detection [1].

Historically, there have been two major categories of coherent communication systems: homodyne and heterodyne. Homodyne detection requires accurate frequency and phase locking of the incoming signal to a carrier, such that the offset frequency is zero. The carrier can be (a) a local oscillator (LO) laser that is generated at the receiver and typically requires an electronic-based phase-locked loop to stabilize the locking of the LO to the incoming signal [4–8]; or (b) a simple frequency tone that may have been sent along with the signal and can be located out of the original signal band or on the orthogonal polarization, thus consuming some bandwidth [9–13].

In [14], a different approach was demonstrated that enabled automatically locked frequency/phase homodyne detection for the incoming data signal without the need for frequency/phase tracking. This scheme uses the optical nonlinearity of PPLN waveguides to generate the signal conjugate, which is coherently added to the signal and the local oscillator [15,16]. This Letter proposes applying this approach to detect wavelength-division multiplexing (WDM) DP-signals. We utilize PPLN waveguides inside polarization-diversity loops (PDL) to achieve the homodyne detection on a DP-signal and then apply multiplexing to enable detection of two single-polarization (SP) WDM channels simultaneously [17,18]. The system exhibits a bit-error rate (BER) below 3.8×10^{-3} for baud rates up to 32 Gbaud when detecting (a) the dual-polarization quadrature phase-shift keyed (QPSK) signal, and (b) two single-polarization binary phase-shift keyed (BPSK) channels up to 20 Gbaud. A summary addresses the requirements and limitations of implementing the system to detect WDM DP-signals based on this homodyne receiver.

The concept of homodyne detection of WDM DP-signals is depicted in Fig. 1. Input WDM DP-QPSK signals $\boldsymbol{S}_i(t) = S_{i,x}(t)\underline{\boldsymbol{x}} + S_{i,y}(t)\underline{\boldsymbol{y}}$ (i: is the channel number), as shown in Fig. 1(a), are sent along with a dual-polarization free-running local oscillator laser $\mathbf{LO}(t) = \mathrm{LO}_x(t)\underline{\boldsymbol{x}} + \mathrm{LO}_y(t)\underline{\boldsymbol{y}}$ into the system such that $\mathbf{LO}(t)$ is at the quasi-phase matching (QPM) frequency of the PPLN waveguide $f_{\mathrm{LO}} = f_{\mathrm{QPM}}$. The signals and LO first propagate through a PDL containing a PPLN waveguide (Stage-1). In this PDL, the two orthogonal polarizations are separated using a polarization beam splitter (PBS) and propagate in opposite directions, in which cascaded second-harmonic generation (SHG) of $\mathbf{LO}(t)$ and difference-frequency

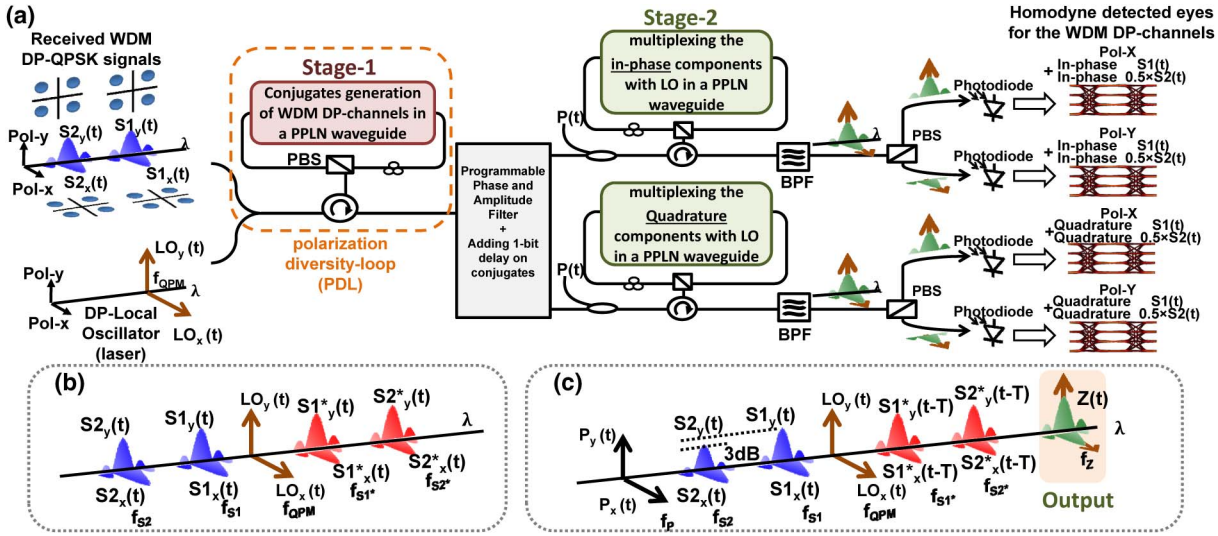

Fig. 1. (a) Concept of homodyne detection of WDM DP-signals utilizing PPLN waveguides inside polarization-diversity loops to coherently multiplex the signals, conjugates, and LO. The generated multi-level eye diagrams at the photodiode outputs correspond to multiplexing the in-phase and quadrature data on both polarization states of the two channels. (b) Conjugates generation in Stage-1 using a dual-polarization LO in a PDL. (c) Multiplexing of the DP-signals, conjugates, and LO using a DP-pump [$P(t)$] and PPLN waveguides inside two PDLs (for the in-phase and quadrature paths) in Stage-2.

generation (DFG) with each $\boldsymbol{S}_i(t)$ generates the conjugates of each signal at each polarization independently. The output of the loop is shown in Fig. 1(b) with conjugates at $f_{\mathrm{Si}*} = 2f_{\mathrm{LO}} - f_{\mathrm{Si}}$ and expressed as $\boldsymbol{S}_i^*(t) = \mathrm{LO}_x^2(t).S_{i,x}^*(t)\underline{\boldsymbol{x}} + \mathrm{LO}_y^2(t).S_{i,y}^*(t)\underline{\boldsymbol{y}}$.

In the next step, a programmable amplitude/phase liquid crystal on silicon (LCoS) filter is used to induce a one-symbol delay (T) between each signal and its conjugate copy. The programmable filter is also used to fine-tune phases and optimize the power levels and add loss of $(0.5)^{i-1}$ on each WDM signal. This loss is needed to obtain multi-level multiplexed eyes at the output. Then, inside Stage-2, two PDLs [for the in-phase (I) and quadrature (Q) paths] perform simultaneous SHG of $\mathbf{LO}(t)$ and sum-frequency generation (SFG) of each signal and its delayed conjugate, which are multiplexed at $2f_{\mathrm{QPM}}$ and, subsequently, converted back to the C-band via DFG using an additional DP-pump $\boldsymbol{P}(t)$. Therefore, the output $\boldsymbol{Z}(t)$ at $f_Z = 2f_{\mathrm{QPM}} - f_P$ as shown in Fig. 1(c) becomes

$$\boldsymbol{Z}(t) \triangleq \Bigg\{ \Bigg[\Bigg(\mathrm{LO}_x^2(t) \cdot \Bigg(\sum_{i=1}^{n} (0.5)^{i-1} \cdot X_{i,x}(t) \Bigg) \underline{\boldsymbol{x}} + \mathrm{LO}_y^2(t) \cdot \Bigg(\sum_{i=1}^{n} (0.5)^{i-1} \cdot X_{i,y}(t) \Bigg) \underline{\boldsymbol{y}} \Bigg) + \left(\mathrm{LO}_x^2(t)\underline{\boldsymbol{x}} + \mathrm{LO}_y^2(t)\underline{\boldsymbol{y}} \right) \Bigg] \cdot \boldsymbol{P}^*(t) \Bigg\}, \tag{1}$$

where $\boldsymbol{X}_i(t) = \boldsymbol{S}_i(t).\boldsymbol{S}_i^*(t-T)$ is the multiplication between the signal and its delayed conjugate; $\boldsymbol{X}_i(t)$ is basically the phase modulated differential data pattern of the channel i and acts as a phase filter that significantly attenuates lower frequency phase noise which is usually the transmitter's laser phase noise. Because laser phase noises are reduced, the system's output data can be considered phase and frequency locked to $\mathbf{LO}^2(t)$ [14–18]. Finally, the output $\boldsymbol{Z}(t)$ is selected via a bandpass filter (BPF) on the I/Q paths, and the polarization states are separated using PBSs and sent onto the photodiodes (square-law detectors) to detect the signal components, in which the eye diagrams will have 2^i levels and the output electrical power is proportional to Eq. (2) for the in-phase component and Eq. (3) for the quadrature component:

$$\left| \mathbf{LO}^2(t) + \sum_{i=1}^{n} (0.5)^{i-1} \cdot \boldsymbol{X}_i(t) \right|^2 \tag{2}$$

$$\left| j \cdot \mathbf{LO}^2(t) + \sum_{i=1}^{n} (0.5)^{i-1} \cdot \boldsymbol{X}_i(t) \right|^2. \tag{3}$$

The experimental setup of single DP-signal detection is shown in Fig. 2(a). Laser-1 at $\lambda_1 = 1535.6$ nm is modulated in a single-polarization nested I/Q Mach–Zehnder modulator (MZM) driven by a $2^{15} - 1$ pseudo-random binary sequence (PRBS) to generate the QPSK signal at 20 and 32 Gbaud. The signal is transformed into a DP-signal $\boldsymbol{S}(t)$ using the emulator

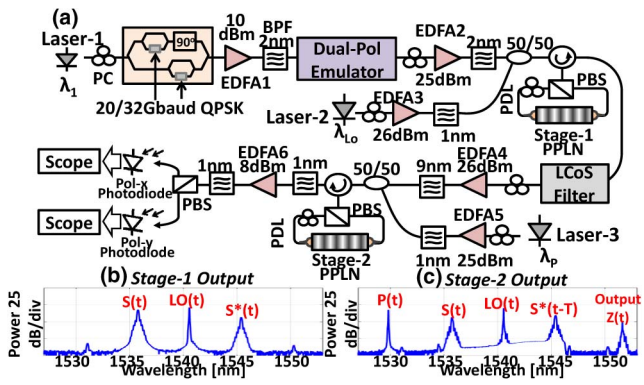

Fig. 2. (a) Experimental setup for a homodyne receiver for a DP-QPSK signal using PPLNs inside a PDL. (b) Experimental spectrum after the first stage (Stage-1). (c) Experimental multiplexing spectrum after Stage-2.

and amplified to 25 dBm using an EDFA2. $\mathbf{LO}(t)$, which originates from Laser-2 at $\lambda_{QPM} = \lambda_{LO} = 1540.3$ nm, is amplified to 26 dBm in EDFA3 and, subsequently, combined with the signal. The BPFs in the experiment have 1–2 dB loss. The signal and LO are sent into Stage-1 to generate the conjugate; the spectrum after the PDL is shown in Fig. 2(b). The signal, LO, and conjugate then go into the LCoS filter to add the one-symbol delay on the conjugate and to adjust the phases before amplification in EDFA4, which is set to 26 dBm. Afterward, a pump $\boldsymbol{P}(t)$ from Laser-3 at $\lambda_P = 1530.6$ nm with 25 dBm power is added using a 50/50 coupler and the output at 1551.6 nm is generated in the second PDL, as shown in the spectrum in Fig. 2(c).

The output is filtered, and the polarization states are separated in a PBS and detected. The eyes are captured using a 32 GHz PIN photodiode which received +8 dBm optical power and was connected to a 50 GHz sampling oscilloscope. The BER measurements are performed by recording the stream using an 80 Gsample/s real-time oscilloscope, in which the threshold is fixed, and the errors are counted. Furthermore, the 0.1 nm OSNR is adjusted and measured prior to EDFA2. This experiment demonstrates the concept of detecting I and Q channels by building only one path with one PPLN waveguide in Stage-2, and we switch between in-phase and quadrature data by adding 45° phase to $\mathbf{LO}(t)$ in the LCoS filter which corresponds to a phase shift of $2 \times 45° = 90°$ on $\mathbf{LO^2}(t)$. However, for full system deployment, we believe that two paths with separate PPLNs are needed to independently multiplex the in-phase and quadrate data with $\mathbf{LO^2}(t)$. Furthermore, the PPLN waveguides should have similar QPM frequencies. In this experiment, the PPLN waveguides are identical, and the QPM frequency was temperature controlled to 90°C throughout the experiment for both waveguides.

The results of this experiment are depicted in Fig. 3. In Figs. 3(a) and 3(b), the captured eyes are shown for the I and Q data up to 32 Gbaud. This figure also shows the detection of inverse data patterns by adding 90° to $\mathbf{LO}(t)$ (180° on $\mathbf{LO^2}(t)$). The BER curves for the system are shown in Fig. 3(c), indicating that the 20 Gbaud channel performed only ~0.5 dB better than the 32 Gbaud case; this difference is observed because the 20 Gbaud case requires a 50 ps delay in the LCoS, which is at the performance edge of that device. Consequently,

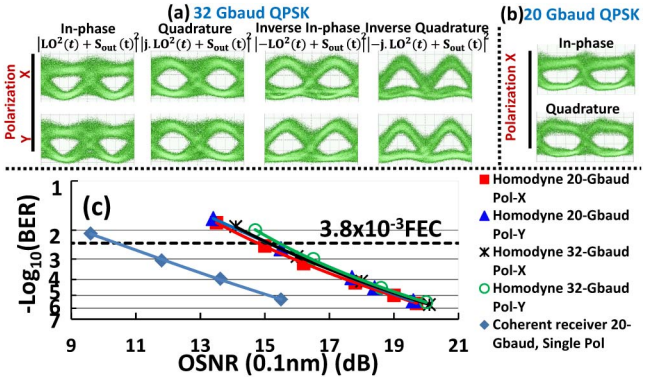

Fig. 3. Experimentally recorded eyes from homodyne detection of a DP-QPSK signal showing the I/Q components under different conditions at (a) 32 Gbaud and (b) 20 Gbaud. (c) BER performance of the homodyne detection system and the BER measured using a coherent receiver.

the signal incurred 1–2 dB of additional loss, and more noise is loaded in the subsequent EDFA.

The system was modified to detect two single-polarization channels using the experimental setup shown in Fig. 4(a). Two lasers (Laser-1 and Laser-2) are modulated using the nested I/Q MZM driven by 10 and 20 Gbaud $2^{15} - 1$ PRBS data to generate the BPSK signals $\boldsymbol{S_1}(t)$ and $\boldsymbol{S_2}(t)$ at $\lambda_1 = 1535.7$ and $\lambda_2 = 1537.3$ nm, respectively. The two data channels are decorrelated by separating them in a wavelength-selective switch (WSS) and then combined using a 50/50 coupler with an additional ~1 meter delay in one path. Signals are amplified to 20 dBm in EDFA2, filtered in a BPF, and then combined with the $\mathbf{LO}(t)$, which originates from Laser-3 at $\lambda_{QPM} = \lambda_{LO} = 1540.4$ nm with a power of 25 dBm. The combined signals and LO are sent into Stage-1. The spectrum after the first nonlinear stage is shown in Fig. 4(b), in which the conjugates of the two signals are generated. Next, the PPLN output is sent into the LCoS filter to adjust phases, add delays to the conjugates, and add a 3 dB loss on $\boldsymbol{S_2}(t)$ compared to $\boldsymbol{S_1}(t)$. In addition, after the amplifier that boosts the LCoS output to 30 dBm in EDFA4, an additional delay between the signals and conjugates is introduced using a short dispersion-compensating fiber (DCF). This delay is added because this experiment uses a 10 Gb/s signal with a 100 ps pulse width, but the LCoS filter delay is limited to ±25 ps. The DCF has a dispersion of 160 ps/nm.km and lengths of 100 and 25 m are used in the 10 and 20 Gbaud experiments, respectively. A pump $\boldsymbol{P}(t)$ from Laser-4 at $\lambda_P = 1530.4$ nm with 20 dBm power is combined with the DCF output and sent into Stage-2 to generate the multiplexed output at 1550.8 nm. The spectrum of the multiplexed output of both channels with the LO is shown in Fig. 4(c). The spectra of the multiplexed outputs of Stage-2, when only one signal and its corresponding conjugate pass the LCoS filter while the other signal/conjugate pair is blocked, are shown in Figs. 4(d) and 4(e).

Results for the simultaneous homodyne detection of two signals are shown in Fig. 5. Figure 5(a) shows the output eyes when only the signal/conjugate pair of signal 1 is passed in the

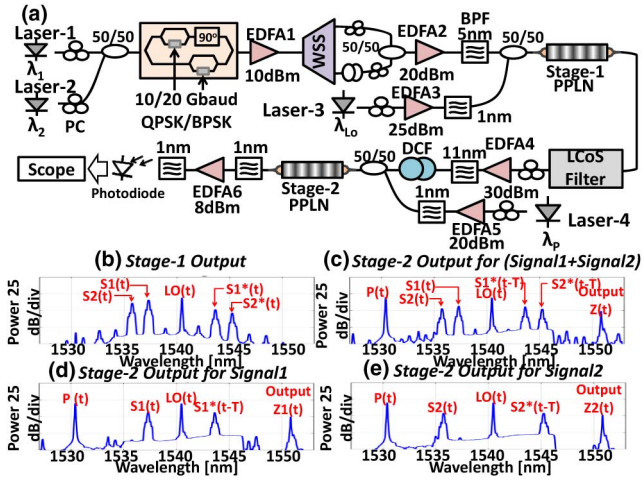

Fig. 4. (a) Experimental setup of homodyne detection for two SP-PSK signals using nonlinearity. (b) Spectrum after conjugate generation in Stage-1. (c) Spectrum of the multiplexing of both signals with LO after Stage-2. (d) and (e) Multiplexing spectra when only one signal/conjugate pair is transmitted at the LCoS filter, while the other pair is blocked.

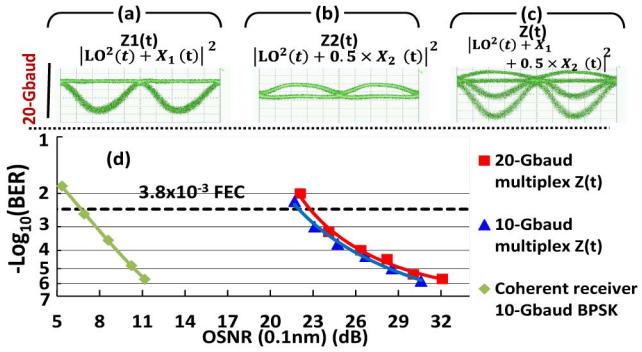

Fig. 5. (a) Experimental homodyne detection eyes for the first BPSK signal. (b) Detected eyes for the second BPSK signal. (c) The multiplexed four-level eyes composed of two BPSK signals at 20 Gbaud. (d) BER performance of the four-level multiplexed output.

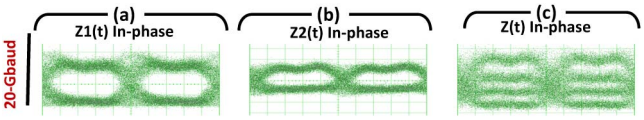

Fig. 6. (a) Homodyne detection of the first QPSK signal in a system of two 20 Gbaud channels (in-phase component). (b) In-phase component of the second QPSK signal. (c) Experimental homodyne detection of the multiplexed two QPSK signals at 20 Gbaud showing noisy eyes with BER exceeding 3.8×10^{-3} due to power handling and conversion efficiencies limitations.

LCoS filter corresponding to the output $\boldsymbol{Z_1}(t)$ in Fig. 4(d). Figure 5(b) shows how the system detects the output $\boldsymbol{Z_2}(t)$, corresponding to the signal/conjugate pair of signal 2 as in the spectrum shown in Fig. 4(e). The next configuration passes all signals and conjugates to yield the four-level multiplexed output at 20 Gbaud shown in Fig. 5(c). The BER of the multiplexed output signals is measured against the OSNR in Fig. 5(d), which confirms that the system can perform below a threshold of 3.8×10^{-3}. For comparison, the BER measured with a coherent receiver for a single 10 Gbaud BPSK signal is also indicated on the plot.

Finally, the detection of two QPSK signals is evaluated. In Figs. 6(a) and 6(b), the detection of each 20 Gbaud QPSK signal when the other signal/conjugate pair is blocked shows that the eyes of both signals get noisier compared to the BPSK experiment; when a multiplexed output of two signals is detected [Fig. 6(c)], the BER exceeds the 3.8×10^{-3} threshold.

This homodyne detection scheme needs to be augmented to fully detect WDM DP-signals. A diversity loop structure is required to process both polarizations concurrently, and that loop is likely to exacerbate the performance degradation issues seen in the detection of two QPSK channels, notably which drive the BER above the FEC threshold. The challenge is the result of the limit of power sent into the PPLN waveguides while avoiding photorefractive damage. Thus, the diversity loop's bidirectionality means that this power limit applies to the sum of the directional components, and each conversion stage needs to be reduced by 3 dB. This can be addressed using nonlinear devices with improved conversion efficiencies that support higher total input power levels (as noted in [19,20]), especially in the first stage, which is operated at 100 mW in this experiment. Raising the PPLN power limit would help to overcome the noise arising from amplifying lower power conjugates in the next stage. Furthermore, the maximum number of channels that can be detected simultaneously here appears to be limited by the additional 3 dB loss needed for each additional channel to achieve 2^i multiplexed eyes. Further, balanced detection as described in [14] might be needed to improve performance, providing an additional gain of up to 3 dB.

In conclusion, this Letter demonstrates automatically locked homodyne detection of a DP-QPSK up to 32 Gbaud and two single-polarized BPSK signals up to 20 Gbaud using two stages of PPLN waveguides with a BER below the FEC threshold, and reports the corresponding eye diagrams.

Funding. Center for Integrated Access Network (CIAN); National Science Foundation (NSF); Defense Security Cooperation Agency (DSCA).

REFERENCES

1. G. P. Agrawal, *Fiber-Optic Communication Systems* (Wiley, 2010).
2. E. Ip, A. P. T. Lau, D. J. F. Barros, and J. M. Kahn, Opt. Express **16**, 753 (2008).
3. S. J. Savory, Opt. Express **16**, 804 (2008).
4. L. G. Kazovsky, J. Lightwave Technol. **4**, 182 (1986).
5. S. Norimatsu and K. Iwashita, J. Lightwave Technol. **9**, 1367 (1991).
6. G. Goldfarb and G. Li, Opt. Express **14**, 8043 (2006).
7. A. Leven, N. Kaneda, U. Koc, and Y. Chen, IEEE Photon. Technol. Lett. **19**, 366 (2007).
8. R. Noé, J. Lightwave Technol. **23**, 802 (2005).
9. T. Miyazaki, IEEE Photon. Technol. Lett. **18**, 388 (2006).
10. S. Shinada, M. Nakamura, Y. Kamio, and N. Wada, Opt. Express **20**, B535 (2012).
11. S. K. Ibrahim, S. Sygletos, R. Weerasuriya, and A. D. Ellis, Opt. Express **19**, 8320 (2011).
12. S. Beppu, K. Kasai, M. Yoshida, and M. Nakazawa, Opt. Express **23**, 4960 (2015).
13. A. Lorences-Riesgo, T. A. Eriksson, A. Fülöp, M. Karlsson, and P. A. Andrekson, in *European Conference on Optical Communication (ECOC)* (2015), paper We.3.6.2.
14. M. R. Chitgarha, A. Mohajerin-Ariaei, Y. Cao, M. Ziyadi, S. Khaleghi, A. Almaiman, J. D. Touch, C. Langrock, M. M. Fejer, and A. E. Willner, J. Lightwave Technol. **33**, 1344 (2015).
15. M. R. Chitgarha, S. Khaleghi, M. Ziyadi, A. Mohajerin Ariaei, A. Almaiman, W. Daab, D. Rogawski, M. Tur, J. Touch, C. Langrock, M. Fejer, and A. Willner, Opt. Lett. **39**, 2928 (2014).
16. M. R. Chitgarha, S. Khaleghi, Z. Bakhtiari, M. Ziyadi, O. Gerstel, L. Paraschis, C. Langrock, M. M. Fejer, and A. E. Willner, Opt. Lett. **38**, 3350 (2013).
17. M. Ziyadi, A. Mohajerin Ariaei, A. Almaiman, Y. Cao, M. R. Chitgarha, P. Liao, Y. Akasaka, J. Yang, M. Sekiya, J. Touch, C. Langrock, M. M. Fejer, M. Tur, and A. Willner, in *Conference on Lasers and Electro-Optics*, OSA Technical Digest (online) (Optical Society of America, 2015), paper STh1O-5.
18. A. Almaiman, M. Ziyadi, A. Mohajerin Ariaei, Y. Cao, M. R. Chitgarha, P. Liao, Y. Akasaka, J. Yang, M. Sekiya, J. Touch, M. Tur, C. Langrock, M. M. Fejer, and A. Willner, in *Conference on Lasers and Electro-Optics*, OSA Technical Digest (online) (Optical Society of America, 2015), paper STh1O-4.
19. T. Umeki, O. Tadanaga, and M. Asobe, IEEE J. Quantum Electron. **46**, 1206 (2010).
20. L. Grüner-Nielsen, S. Dasgupta, M. D. Mermelstein, D. Jakobsen, S. Herstrøm, M. E. V. Pedersen, E. L. Lim, S. Alam, F. Parmigiani, D. Richardson, and B. Pálsdóttir, in *European Conference on Optical Communication (ECOC)* (2010), paper Tu.4.D.3.